ELSEVIER

Magnetic Resonance Imaging, Vol. 14, No. 10, pp. 1157–1163, 1996

0730-725X/96 $15.00 + .00

PII S0730-725X(96)00219-0

● *Original Contribution*

QUANTIFICATION AND IMPROVEMENT OF THE SIGNAL-TO-NOISE RATIO IN A MAGNETIC RESONANCE IMAGE ACQUISITION PROCEDURE

J. SIJBERS,* P. SCHEUNDERS,† N. BONNET,‡ D. VAN DYCK,† AND E. RAMAN*

*Biomedical Physics and †Vision Lab, Department of Physics, RUCA University of Antwerp, 2020 Antwerp, Belgium, and ‡Unité INSERM 314, Université de Reims, Reims, France

A procedure is developed to quantify and improve the signal-to-noise ratio (SNR) of magnetic resonance images. The image SNR is quantified using the correlation function of two independent acquisitions of an image. To test the performance of the quantification, SNR measurement data are fitted to theoretically expected curves. The proposed correlation technique is also used to improve the SNR by estimating the amplitude of the signal spectrum. The technique is applied to a set of MR images, and its performance in terms of gain in SNR, contrast-to-noise ratio (CNR), and resolution loss is compared to that of classical noise filters. The SNR as well as the CNR is improved significantly with minor loss of resolution. Finally, it is shown that the correlation technique can be implemented in a highly efficient way in almost any acquisition procedure of a magnetic resonance imaging system.

Keywords: **Signal-to-noise ratio; Correlation function; Multiple magnetic resonance image acquisitions.**

INTRODUCTION

Many image acquisition procedures [magnetic resonance imaging (MRI), positron emission tomography, single photon emission computer tomography (SPECT), etc.] suffer from image degradation by noise. For MRI the primary source of random noise is thermal noise, which forms a statistically independent random source entering the MR data in the time domain. Thermal noise is white and can be characterized by a Gaussian random field with zero mean and constant variance.[1] Therefore, the noise is not correlated with the signal or with itself. Apart from thermal noise, structured noise usually degrades the image quality as well, owing to MR system characteristics, physiological pulsations, or object motion. Recently, Buonocore et al.[2] developed a data-processing algorithm based on least-mean-squared adaptive filtering to suppress structured noise in MR images; the algorithm, however, retains the contribution of random noise. In this article we assume the MR image to be corrupted only by random noise.

Quantification of the signal-to-noise ratio (SNR) is important for several reasons. First, it provides a measure for the image quality in terms of image details. Second, besides testing different system parameters such as main magnetic field homogeneity or DC offset between the real and imaginary signal components, the SNR can be used to check the performance of the MR system itself. Because the MR signal and, hence, the SNR strongly depend on the field homogeneity, the shape of the radiofrequency (RF) pulses, the stability of the RF amplifiers, etc., quantification of the SNR is a useful tool in the analysis of the MR system. For this purpose, usually the SNR is determined on images of a specially constructed phantom object at regular intervals.

A common way to estimate the amount of noise in an image is by subtracting two acquisitions of the same object and calculating the standard deviation (SD) of the resulting image.[3] Murphy et al.[4] elaborated on this technique further and used a parallel rod test object for SNR measurements from the signal and nonsignal blocks. Alternatively, the SNR can be measured directly from the noise of a large uniform signal or from

RECEIVED December 23, 1995; ACCEPTED June 8, 1996.
Address correspondence to Jan Sijbers, University of Antwerp, Department of Physics, Groenenborgerlaan 171, B-2020 Antwerp, Belgium.

nonsignal regions.[5] Although this method may lead to useful estimates of the SNR, large homogeneous regions are often hard to find. Both techniques estimate the SNR from magnitude MR images, where the noise is Rayleigh distributed; such calculations must be done with care.[6] In another approach, it has been suggested that a cross-correlation technique could be used to estimate the SNR of band-limited stochastic functions.[7] This technique has been exploited in the field of electron microscopy.[8,9] In this study, we introduce the correlation technique in MRI to quantify the SNR directly from the time domain data by cross-correlating two acquisitions of the same MR image.

The problems of quantification and improvement are highly related to each other, since to quantify the SNR, one must be able to separate the noise from the signal. A well-known and widely used procedure to improve the counting statistics of MR imaging and, hence, of the SNR is time integration. By averaging over N consecutive images, the SNR improves with $N^{1/2}$. The main advantage of this technique is the gain in SNR without any loss of spatial resolution, assuming a perfect geometrical registration of all the images. Nevertheless, to obtain high-quality images, uneconomically large acquisition times are sometimes required. Despite the progress of fast imaging techniques (echo planar imaging, fast low angle shot, and fast spin echo) there are situations in which multiple averaging is not acceptable, such as three-dimensional (3D) imaging or dynamic studies such as diffusion processes. Therefore, classical techniques such as spatial averaging and low-pass or median filters are usually applied to the noisy image to increase the SNR.[10,11]

Bonnet[12] showed that from two acquisitions of the same image, both corrupted with additive uncorrelated noise, the SNR can be improved significantly by correlating both acquisitions and estimating the amplitude of the signal spectrum. In this work we compare the performance of classical filters with that of the correlation filter. The correlation technique is very useful in the case of MR images, as these are acquired in the Fourier domain. Because of the correlation theorem, it is favorable in terms of processing time to perform a correlation of images in the Fourier domain, which makes the technique extremely suited for implementation in a highly efficient way in many MR image acquisition procedures.

The outline of this article is as follows. In the next section, the theory of the correlation technique is outlined. In the third section, two experiments are described in which the accuracy and precision of the SNR quantification are tested. In addition the performance of the correlation filter in terms of gain in SNR, contrast-to-noise ratio (CNR) and loss of resolution are compared with corresponding classical filters. The image resolution and SNR are calculated on the total image, but a smaller region of interest (ROI) can also be taken. The results of the experiments are reported in the last section. Finally, a practical way of implementing the SNR in an MR image acquisition procedure is discussed.

THEORY

In this section, we outline the theory for quantification and improvement of the SNR. In the description of the methods, we assume the MR imaging process to be stationary (i.e., the statistical properties of two images, acquired at different times, are equal).[13] Although the extension to higher dimensions is straightforward, we will proceed now for the 2D case.

We assume that an experimental MR image i consists of a signal s corrupted by additive, uncorrelated noise n with zero mean ($<n> = 0$). The signal s includes possible blurring caused by the system point spread function:

$$i(x,y) = s(x,y) + n(x,y) \quad (1)$$

where (x,y) denotes the MR image point. As a definition of the SNR, the ratio of the signal SD to the noise SD is chosen:

$$SNR = \sqrt{\frac{\sigma_s^2}{\sigma_n^2}} \quad (2)$$

We prefer the SD of the signal in the numerator of Eq. (2) above the signal mean because this choice takes more account of the information content in the image. The SNR as defined above cannot be determined exactly from one experimental acquisition only. However, it has been shown[7] that in the case of uncorrelated, additive noise, two consequent acquisitions i_1 and i_2

$$\begin{aligned} i_1(x,y) &= s(x,y) + n_1(x,y) \\ i_2(x,y) &= s(x,y) + n_2(x,y) \end{aligned} \quad (3)$$

can be used to quantify the SNR. The cross-correlation function (CCF) of the two images becomes:

$$i_1 \otimes i_2 = s \otimes s + n_1 \otimes s + s \otimes n_2 + n_1 \otimes n_2 \quad (4)$$

Since the noise is uncorrelated, one has

$$n_1 \otimes s = s \otimes n_2 = n_1 \otimes n_2 = 0 \tag{5}$$

so that

$$i_1 \otimes i_2 = s \otimes s \tag{6}$$

i.e., the CCF of the two images is equal to the autocorrelation function (ACF) of the signal. This observation is used in the cross-correlation coefficient (CCC) which is defined as:

$$\rho(x,y) = \frac{i_1(x,y) \otimes i_2(x,y) - \langle i_1 \rangle \langle i_2 \rangle}{\sigma_1 \sigma_2} \tag{7}$$

where $\langle i_1 \rangle$, $\langle i_2 \rangle$, σ_1, and σ_2 are, respectively, the mean and SD of the two MR images i_1 and i_2. The SNR can be computed from the maximum of the CCC. When the two acquisitions are perfectly registered (no shift of the sample has occurred), this maximum occurs in the center of the CCC:

$$\rho_m = \frac{\langle i_1 i_2 \rangle - \langle i_1 \rangle \langle i_2 \rangle}{\sqrt{[\langle i_1^2 \rangle - \langle i_1 \rangle^2][\langle i_2^2 \rangle - \langle i_2 \rangle^2]}} \tag{8}$$

or, using Eq. (6):

$$\rho_m = \frac{\langle s^2 \rangle - \langle s \rangle^2}{\sqrt{[\langle s^2 \rangle - \langle s \rangle^2 + \langle n_1^2 \rangle^2] \times [\langle s^2 \rangle - \langle s \rangle^2 + \langle n_2^2 \rangle^2]}} \tag{9}$$

which finally results in the following simple expression:

$$\rho_m = \frac{\sigma_s^2}{\sigma_s^2 + \sigma_n^2} \tag{10}$$

From this the expression for the SNR simply becomes:

$$SNR = \sqrt{\frac{\rho_m}{1 - \rho_m}} \tag{11}$$

Notice that the subtraction of $\langle i_1 \rangle \langle i_2 \rangle$ in the numerator along with the denominator make the SNR measurement insensitive for differences in scaling constants between the two MR images. Remark also that ρ_m can be calculated completely in the Fourier domain. Indeed, using Parseval's theorem, one obtains from Eq. (8):

$$\rho_m = \frac{\langle I_1 I_2^* \rangle - I_1(0,0) I_2(0,0)}{\sqrt{[\langle I_1^2 \rangle - I_1^2(0,0)][\langle I_2^2 \rangle - I_2^2(0,0)]}} \tag{12}$$

I and I^* are, respectively, the complex raw MR data and their complex conjugate. The coordinate (0,0) represents the center of the CCC. Equation (12) allows the SNR of the MR image to be calculated directly from the raw MR data. In this way, the SNR can be predicted before the Fourier transformation takes place.

The property that the CCF of two acquisitions of the same MR image reduces to the ACF of the noiseless image can also be exploited to improve the SNR. The Fourier spectrum of the CCF leads to an estimate of the signal power spectrum $|S(u,v)|^2$ with

$$|S(u,v)|^2 = \frac{I_1(u,v) I_2^*(u,v) + I_1^*(u,v) I_2(u,v)}{2} \tag{13}$$

where (u,v) denotes the raw data point. If the acquisitions I_1 and I_2 were not corrupted by noise, the power spectrum would be positive everywhere. However, owing to the noise, some points in the estimated spectrum may become negative and are therefore forced to zero. This procedure is preferred above operations such as averaging or replacing negative pixel values by neighboring pixel values, because these create additional unwanted frequency information. From Eq. (13) an estimate for the complex signal spectrum is derived:

$$S_F(u,v) = \sqrt{|S(u,v)|^2}\, e^{j\Phi(u,v)} \tag{14}$$

where Φ is the phase of the averaged complex image $(I_1+I_2)/2$. As was pointed out by Bonnet,[12] another estimate of the signal spectrum is given by:

$$S_W(u,v) = \frac{|S(u,v)|^2}{|I(u,v)|} e^{j\Phi(u,v)} \tag{15}$$

which is obtained by using a Wiener filter combined with the correlation procedure. This estimate leads to the best result in a least-squared sense. Hence, this filter is especially recommended for images corrupted by Gaussian noise.

The method can be applied to the images provided perfect geometrical registration. If the acquisitions are not perfectly registered, the maximum of the CCF will generally decrease, which leads to an underestimation of the SNR. However, the CCF maximum will not be affected if the images differ from a uniform translational shift, and hence, the SNR estimate is still valid. SNR improvement as described above may cause additional blurring in the case of misregistration. Nevertheless, uniform geometrical registration can easily be performed by examining the position of the CCF maximum. In this way, subpixel registration can even be achieved by, for instance, bilinear interpolation.

MATERIALS AND METHODS

MR images were obtained on either an Oxford Biospec imaging system with a horizontal bore of 26.5 cm, a magnetic field strength of 1.9 T, and a maximal gradient strength of 0.01 T/m; or on an SMIS MRI apparatus with a horizontal bore of 8 cm, a field strength of 7 T, and a maximal gradient strength of 0.2 T/m. Test images were acquired at room temperature from a phantom object, a water-filled rod using a birdcage RF coil. The in-plane spatial resolution was 60 μm in both directions, and slice thickness was 1 mm.

The following experiments were set up to test the performance of the SNR quantification and the SNR improvement of the correlation technique. For implementation of the outlined techniques, two routines were developed, one using Eqs. (11) and (12), which compute the SNR, and one using Eqs. (14) and (15) to improve the SNR.

The validity of the quantification of the SNR is tested by averaging N identical MR acquisitions of the phantom object and checking the expected linear behavior of $(\mathrm{SNR})^2$ with respect to N. A spin-echo (SE) pulse sequence was used with repetition time (TR) = 1 s and echo time (TE) = 24 ms. An image of the phantom was obtained after averaging N equal acquisitions. A second image was acquired with the same imaging parameters. From the two resulting images, the SNR is calculated using Eqs. (11) and (12). This procedure is repeated for different values of N.

Furthermore, the precision of the SNR quantification is tested. This is done by determining the spin-lattice relaxation time T_1 of free water from two independent experiments: first from the power spectrum height as a function of the inversion time TI; and second, directly from the phantom image SNR, calculated with the cross-correlation method described above. In this way a possible bias in the SNR quantification can be detected.

In the first experiment, the exponential saturation of the signal is measured using an inversion recovery pulse sequence. The amplitude of the free induction decay (FID) spectrum is plotted as a function of the inversion time (IT). Afterward, the T_1 relaxation time is estimated by fitting the data to the function:

$$SNR \sim N[H](1 - 2e^{-\mathrm{TI}/\mathrm{T}_1}) \qquad (16)$$

where $N[H]$ is the proton density of free water.

In the second experiment, we calculated the SNR of 30 images of the same phantom which are taken with incrementally larger TI's. A fast imaging sequence (SNAPSHOT FLASH) is used for this experiment. To minimize the influence of the spin–spin relaxation (T_2), the smallest possible echo time, TE = 1.7 ms, was chosen. Because only the signal SD of the acquired images changes with TI, the SNR data are expected to follow Eq. (16). From these data, the T_1 parameter can again be estimated. In both experiments, the theoretical curve [see Eq. (16)] is fitted to the data using a two-parameter least-squares fit.

The applicability of enhancing the SNR of MR images of realistic objects is tested in the following experiment. Four independent acquisitions of the same MR image of a cucumber are acquired (TR = 1 s; TE = 30 ms) with an in-plane resolution of 0.4 mm and slice thickness of 2 mm. The images are 2 × 2 correlated and the signal spectrum is estimated from the two final images using Eq. (13), after which the SNR is calculated. The results are compared with the averaging procedure. Hereby, the four acquisitions are 2 × 2 averaged, and on the two resulting images the SNR is again estimated using Eqs. (11) and (12). Moreover, we compared our filtered images with the median filter which is known to be an edge-preserving filter. The reason for choosing the median filter is that its performance is based only on the size of the mask (4-connected, 8-connected, etc.), whereas other edge-preserving filters (e.g., σ filter) need additional prior information such as the image SNR.

In addition to the SNR measurements of the filtered image, the CNR for two distinct regions in the image is computed, because this parameter is more important to visualization. The CNR is defined as:

$$CNR = \frac{\langle s_a \rangle - \langle s_b \rangle}{\sigma_n} \qquad (17)$$

where $\langle s_a \rangle$ and $\langle s_b \rangle$ denote the mean signal of regions a and b, respectively. The noise SD can be derived from Eq. (6):

$$\sigma_n^2 = \left[\frac{i_1 \otimes i_1 + i_2 \otimes i_2}{2} - i_1 \otimes i_2 \right]_{\max} \qquad (18)$$

The CNR is expected to increase with the same factor as the SNR, because the improvement is based on the decrease of the noise power with only minor signal modifications. To test this hypothesis, two homogeneous regions, the seeds and the pulp, were selected from the cucumber image, after which the CNR was calculated for different filtered images, thereby using the same ROIs.

The loss of resolution, which is an expected side effect of improving the SNR with any noise filter, is measured by estimating the image resolution. This estimate is derived from two acquisitions of a noisy image[14,15]: it is given by the area at half-maximum of the CCF. The larger this area is, the larger is the separation of object points that cannot be distinguished in the image. Because the improvement of the SNR results in a rather uniform degradation of the image resolution, the area at half maximum of the CCF is qualitatively a reliable measure for the loss of spatial resolution.

To test the performance of the proposed techniques, we calculate the CCF areas of the MR images after application of the correlation technique. Here we use the CCF area of the original images as a reference resolution measure (0% loss of resolution). The finite size of this area is due to the correlations in the object. A 50% loss of resolution is obtained by applying a 2 × 2 spatial average filter in which each pixel of the image is replaced by the average value of a 2 × 2 neighborhood of that pixel. We compared the performance of the correlation techniques with the 2 × 2 spatial average and the median filter. For each filtered image, the image SNR is measured with the cross-correlation method described above.

RESULTS AND DISCUSSION

As can be observed clearly from Fig. 1, the SNR improves linearly with the square root of the number of acquisitions, indicating an accurate quantification of the image SNR. Statistically the accuracy is proportional to the square root of the number of data points. From independent SNR measurements of 50 acquisitions of the same image, the relative error of the SNR value for a 256 × 256 image was found to be within 2%. Here the relative error is defined as the SD of the SNR divided by the mean SNR. It is clear that the

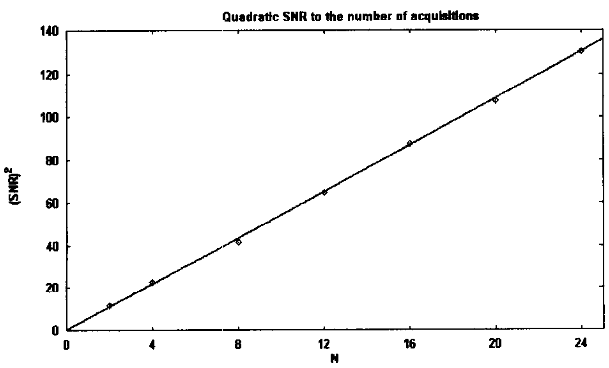

Fig. 1. The $(\mathrm{SNR})^2$ as a function of N, the number of acquisitions.

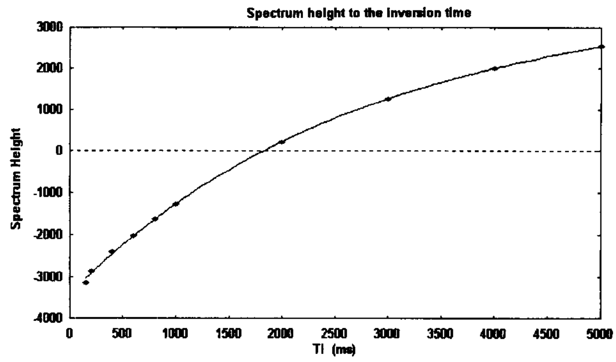

A

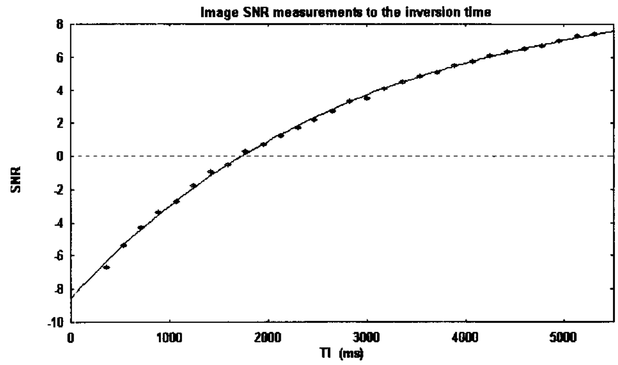

B

Fig. 2. (a) Measurements of the FID's amplitude as a function of TI. (b) SNR measurements from T_1-weighted images as a function of TI.

outlined method to quantify the SNR will even be much more precise for 3D images.

Figure 2a shows the results for the T_1 measurements of water from the amplitude of the FID. The data fitting to the theoretical curve of Eq. (16) reveal a T_1 value of (2800 ± 110) ms. This value is confirmed from the SNR measurements of images which are taken with incrementally larger TI values. From Fig. 2b, in this case the exponentional saturation of the SNR is clearly observed. The data fitting reveal a T_1 relaxation time of (2880 ± 90) ms. The observation that the T_1 values obtained from two independent experiments are equal indicates that there is no bias in the quantification of the SNR.

We have observed that with the correlation method, the SNR improves with almost a factor of 2. The SNR of the unprocessed images was 3.24. Figure 3a shows one of the four acquisitions of the original image. Figure 3b is the average of the two acquisitions with an SNR of 4.57. The results after improvement using Eqs. (14) and (15) are displayed in Fig. 3c and 3d, respectively. The SNR is 5.57 and 6.03, respectively. With Eqs. (14) and (15), the upper limit of the gain in SNR is determined by the Fourier phase, which is obtained from the average of the two input images. Hence, the phase image is necessarily polluted by noise. Until now we had not found a better way to reduce the noise contributions in the Fourier-phase image.

As can be observed from the images in Fig. 3, the correlation method improves the SNR but simultaneously decreases the image resolution. This blurring effect occurs with all noise-reducing techniques. In this procedure, it is caused by forcing the negative values of the estimated signal power spectrum to zero. Note that the image-averaging procedure does not suffer from this blurring effect.

In Table 1, the gain in SNR and CNR along with the estimated value for the loss of resolution are shown for a noisy image, the average of two acquisitions, and for images processed with a 4-connected median filter and the proposed correlation techniques. For comparison we included the results for a 2 × 2 spatial averaging filter. The substantial gain in SNR of this filter goes along with an unacceptable loss of resolution. The loss of resolution due to this filter is used as a reference. Although no decrease of resolution is observed for the time-averaging procedure, this technique results in only a small gain of SNR. From this table, one can also observe that the results of the correlation techniques are superior compared with those of the median filter in terms of the loss of resolution. In addition, the proposed correlation techniques have an advantage over the median filter in that the processing time is minimal (i.e., it is implementable in a very efficient way in the Fourier domain, as was elaborated in the previous section).

Table 1. Comparison of the SNR, CNR, and loss of resolution

	SNR	CNR	Resolution loss (%)
Noisy image	3.24	2.93	0
Averaged	4.57	4.16	0
Median filter	5.78	5.26	40
Correlated	5.57	5.04	24
Wiener correlated	6.03	5.55	26
Average filter (2 × 2)	6.41	5.78	50

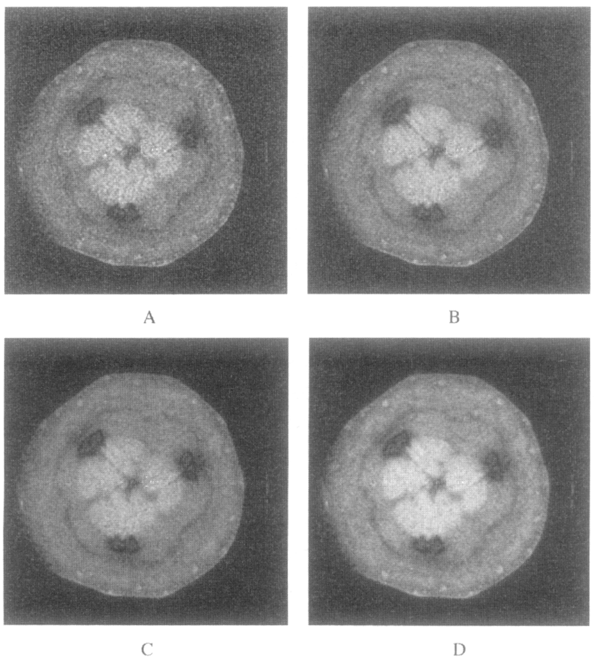

Fig. 3. (a) One of the acquisitions of the original image; (b) average of two acquisitions; (c) improved image, using the correlation technique; (d) improved image, using the modified Wiener approach.

Finally, we suggest using the SNR quantification technique as an on-line evaluation of image quality in terms of random noise. The next strategy could be followed during an MRI procedure. Instead of directly averaging multiple acquisitions to increase the SNR, the acquisitions are stored in two equal sets on the disk and are averaged separately. Each time a new pair of acquisitions is obtained, the SNR of the two sets averaged so far is measured. At the end, the two sets are either averaged again or additionally improved, thus allowing minor loss in resolution.

It must be stressed that both techniques, quantification and improvement, are independent of the way k-space was sampled during acquisition (independent of the pulse sequence, field of view, number of phase-encoding steps, etc.). As a consequence, the described techniques can be implemented in any pulse sequence.

CONCLUSION

In this article we showed that by cross-correlating two acquisitions of the same image, the quantification of the image SNR can be performed in a very accurate way. In addition, the correlation technique can also be used to improve the image SNR significantly with relative minor loss in resolution. Finally, both quantification and improvement can be implemented in an efficient way in many MRI acquisition procedures.

Acknowledgements—The authors thank A. Van der Linden, J. Wright, D. Guilfoyle, and G. Nayler for many helpful suggestions and detailed comments. In addition, they express their appreciation to Johan Van Audekerke for his guidance in the setup of the experiments.

REFERENCES

1. Wang, Y.; Lei, T. Statistical analysis of MR imaging and its applications in image modeling. In: Proceedings

of the IEEE International Conference on Image Processing, Vol. 1.; 1994: 866–870.

2. Buonocore, M.H.; Maddock, R.J.; Antognini, J.F. Algorithm to suppress structured noise in functional neuroimaging. In: Book of abstracts: Proceedings of the Society of Magnetic Resonance Nice, France, Vol. 1; 1995: 237.
3. Sano, R.M.; NEMA standards. Performance standards for clinical magnetic resonance systems. In: R.L. Dixon (Ed). MRI Acceptance Testing and Quality Control—The Role of the Clinical Medical Physicist. Madison, WI: Medical Physics; 1988: pp. 185–189.
4. Murphy, B.W.; Carson, P.L; Ellis, J.H; Zhang, Y.T.; Hyde, R.J; Chenevert, T.L. Signal-to-noise measures for magnetic resonance imagers. Magn. Reson. Imaging 11:425–428; 1993.
5. Kaufman, L.; Kramer, D.M.; Crooks, L.E.; Ortendahl, D.A. Measuring signal-to-noise ratios in MR imaging. Radiology 173:265–267; 1989.
6. Henklemen R.M. Measurement of signal intensities in the presence of noise in MR images; Med. Phys. 12:232–233; 1985.
7. Lenz, F. Electron Microscopy in Material Science. London: Academic; 1971.
8. Frank, J.; Ali-Ali, L. Signal-to-noise ratio of electron micrographs obtained by cross correlation. Nature 256:376–379; 1975.
9. Bonnet, N.; Lebonvallet, S.; El Hila, H.; Colliot, G.; Beorchia, A. Quantitative evaluation of the signal-to-noise ratio and of its improvement (or degradation) by digital filters. J. Phys. 1:1349–1358; 1991.
10. Gonzalez, R.C.; Woods, R.E. Digital Image Processing. New York: Addison Wesley; 1992.
11. Jain, A.K. Fundamentals of Digital Image Processing. Englewood Cliffs, NJ: Prentice-Hall; 1989.
12. Bonnet, N. On the use of correlation functions for improving the image signal-to-noise ratio. Optik 80:103–106; 1988.
13. Papoulis, A. Probability, Random Variables and Stochastic Processes. New York: McGraw-Hill; 1984.
14. Al-Ali, L.; Frank, J. Resolution estimation in electron microscopy. Optik 58:31–40; 1980.
15. Frank, J. A practical resolution criterion in optics and electron microscopy. Optik 43:25–34; 1975.